Measurements of $t\bar{t}$ spin correlations and top-quark polarization using dilepton final states in pp collisions at $\sqrt{s} = 7\,\text{TeV}$

The CMS Collaboration
CERN
(Dated: November 7, 2013)

Spin correlations in the $t\bar{t}$ system and the polarization of the top quark are measured using dilepton final states produced in pp collisions at the LHC at $\sqrt{s} = 7\,\text{TeV}$. The data correspond to an integrated luminosity of $5.0\,\text{fb}^{-1}$ collected with the CMS detector. The measurements are performed using events with two oppositely charged leptons (electrons or muons), a significant imbalance in transverse momentum, and two or more jets, where at least one of the jets is identified as likely originating from a b quark. The spin correlations and polarization are measured through asymmetries in angular distributions of the two selected leptons, unfolded to the parton level. All measurements are found to be in agreement with predictions of the standard model.

Spin correlations in the $t\bar{t}$ system provide direct access to the properties of the bare top quark, as well as a test of the viability of perturbative quantum chromodynamics (QCD) in the $t\bar{t}$ production process [1]. The polarization of the top quarks in $t\bar{t}$ events is another topic of major interest. In the standard model (SM), top quarks are produced with a small amount of polarization that can be attributed to electroweak corrections to the QCD-dominated production process. For models beyond the SM, couplings of the top quark to new particles can alter both the polarization of the top quark and the amount of spin correlation in the $t\bar{t}$ system [2].

At the Tevatron, the top-quark mass has been measured as $m_t = 173.20 \pm 0.87$ GeV [3], and its decay width is $\Gamma_t = 2.0^{+0.7}_{-0.6}\,\text{GeV}$ [4]. This implies a lifetime much shorter than the spin decorrelation timescale of m_t/Λ^2_{QCD} [5]. Consequently, the information about the spin of the top quark at production is transferred directly to its decay products and can be accessed from their angular distributions.

At the Large Hadron Collider (LHC), top quarks are produced abundantly, mainly in pairs. For low $t\bar{t}$ invariant masses, the production is dominated by the fusion of pairs of gluons with the same helicities, resulting in the creation of top-quark pairs with antiparallel spins. At larger invariant masses, the dominant production is via the fusion of gluons with the opposite helicities, resulting in $t\bar{t}$ pairs with parallel spins. These have the same configuration as $t\bar{t}$ events produced via $q\bar{q}$ annihilation [5].

In the decay $t\bar{t} \to \ell^+\nu b\ell^-\bar{\nu}\bar{b}$, in the laboratory frame, the difference in azimuthal angles of the charged leptons ($\Delta\phi_{\ell^+\ell^-}$) is sensitive to $t\bar{t}$ spin correlations, and can be measured precisely without reconstructing the full event kinematics [5]. The top-quark spin can be studied using θ_ℓ, which is the angle of the charged lepton in the rest frame of its parent top quark or antiquark, measured in the helicity frame (i.e., relative to the direction of the parent quark in the $t\bar{t}$ center-of-momentum frame). The CDF, D0, and ATLAS spin correlation and polarization measurements used template fits to angular distributions and observed results consistent with SM expectations [6–11]. In this analysis, the measurements are made using angular asymmetry variables unfolded to the parton level, allowing direct comparisons between the data and theoretical predictions.

The top-quark polarization P in the helicity basis is given by $P = 2A_P$, where the asymmetry variable A_P is defined as

$$A_P = \frac{N(\cos(\theta_\ell) > 0) - N(\cos(\theta_\ell) < 0)}{N(\cos(\theta_\ell) > 0) + N(\cos(\theta_\ell) < 0)}.$$

Here the numbers of events N are counted using the θ_ℓ measurements of both positively and negatively charged leptons (θ_{ℓ^+} and θ_{ℓ^-}), assuming CP invariance.

For $t\bar{t}$ spin correlations, the variable

$$A_{\Delta\phi} = \frac{N(\Delta\phi_{\ell^+\ell^-} > \pi/2) - N(\Delta\phi_{\ell^+\ell^-} < \pi/2)}{N(\Delta\phi_{\ell^+\ell^-} > \pi/2) + N(\Delta\phi_{\ell^+\ell^-} < \pi/2)}$$

provides excellent discrimination between correlated and uncorrelated t and $\bar{t}$ spins, while the variable

$$A_{c_1c_2} = \frac{N(c_1 \cdot c_2 > 0) - N(c_1 \cdot c_2 < 0)}{N(c_1 \cdot c_2 > 0) + N(c_1 \cdot c_2 < 0)},$$

where $c_1 = \cos(\theta_{\ell^+})$ and $c_2 = \cos(\theta_{\ell^-})$, provides a direct measure of the spin correlation coefficient C_{hel} using the helicity angles of the two leptons in each event: $C_{\text{hel}} = -4A_{c_1c_2}$ [12].

The results presented in this Letter are based on data that correspond to an integrated luminosity of $5.0\,\text{fb}^{-1}$ of proton-proton collisions at $\sqrt{s} = 7\,\text{TeV}$, provided by the LHC and recorded by the Compact Muon Solenoid (CMS) detector in 2011.

The central feature of the CMS apparatus is a superconducting solenoid, 13 m in length and 6 m in diameter, which provides an axial magnetic field of 3.8 T. The bore of the solenoid is outfitted with a variety of particle detection systems. Charged-particle trajectories are measured with the silicon pixel and strip trackers that cover a pseudorapidity region of $|\eta| < 2.5$, where η is defined as $\eta = -\ln[\tan\theta/2]$, with θ being the polar angle of the trajectory of the particle with respect

to the counterclockwise-beam direction. A crystal electromagnetic calorimeter and a brass/scintillator hadron calorimeter surround the inner tracking volume and provide high-resolution measurements of energy used to reconstruct electrons, photons, and particle jets. Muons are measured in gas-ionization detectors embedded in the flux return yoke of the solenoid. The detector is nearly hermetic, thereby providing reliable measurements of momentum imbalance in the plane transverse to the beams. A two-tier trigger system selects the most interesting collisions for analysis. A more detailed description of the CMS detector is given in Ref. [13].

For this analysis, pp collisions are selected using triggers that require the presence of at least two leptons (electrons or muons) with large transverse momentum (p_{T}). Electron candidates [14] are reconstructed by associating tracks from the inner tracker with energy clusters in the electromagnetic calorimeter. Muon candidates [15] are reconstructed by combining information from the outer muon detector with the tracks reconstructed by the inner tracker. Additional lepton identification criteria are applied for both lepton flavors in order to reject hadronic jets that are misidentified as leptons [14, 15]. Both electrons and muons are required to be isolated from other activity in the event. This is achieved by imposing a maximum value of 0.15 on the ratio of the scalar sum of supplementary track p_{T} and calorimeter transverse energy deposits within a cone of $\Delta R \equiv \sqrt{(\Delta\eta)^2 + (\Delta\phi)^2} < 0.3$ around the lepton candidate direction, to the transverse momentum of the candidate.

Event selection is applied to reject events other than those from $t\bar{t}$ in the dilepton final state. Events are required to have exactly two opposite-sign, isolated leptons (e^+e^-, $\mu^+\mu^-$, or $e^\pm\mu^\mp$). The electrons (muons) are required to have $p_{\mathrm{T}} > 20\,\mathrm{GeV}$ and to lie within $|\eta| < 2.5$ (2.4). The reconstructed lepton trajectories must be consistent with a common interaction vertex. Events with an e^+e^- or $\mu^+\mu^-$ pair with invariant mass between 76 and 106 GeV or below 20 GeV are removed to suppress Drell–Yan and heavy-flavor resonance production. The jets and the momentum imbalance in each event are reconstructed using a particle-flow technique [16]. The anti-k_{T} clustering algorithm [17] with a distance parameter of 0.5 is used for jet clustering. Corrections are applied to the energies of the reconstructed jets, based on the results of simulations and studies using exclusive dijet and γ+jet data [18]. At least two jets with $p_{\mathrm{T}} > 30\,\mathrm{GeV}$ and $|\eta| < 2.5$, separated by $\Delta R > 0.4$ from leptons passing the analysis selection, are required in each event. At least one of these jets must be consistent with the decay of heavy-flavor hadrons (a "b jet"), identified by the combined secondary vertex b-tagging algorithm [19]. This is based on the reconstruction of a secondary decay vertex, and gives a b-tagging efficiency of about 70% (depending on jet p_{T} and η) with misidentification probabilities of approximately 1.5% and 20% for jets originating from light partons (u, d, and s quarks, and gluons) and c quarks, respectively. The missing transverse energy, $E_{\mathrm{T}}^{\mathrm{miss}}$, is defined as the magnitude of the momentum imbalance, which is the negative of the vector sum of the momenta of all reconstructed particles in the plane transverse to the beam. The $E_{\mathrm{T}}^{\mathrm{miss}}$ in the event is required to exceed 40 GeV in events with same-flavor leptons, in order to suppress the Drell–Yan background.

Simulated $t\bar{t}$ events are generated using MC@NLO 3.41 [20], with a top-quark mass of 172.5 GeV, and showered and fragmented using HERWIG 6.520 [21]. Simulations with different values of m_t and the factorization and renormalization scales are produced in order to evaluate the associated systematic uncertainties.

The dilepton $t\bar{t}$ selection classifies events with τ leptons as signal only when the τ decays leptonically. Other $t\bar{t}$ topologies, such as the lepton+jets and all-hadronic decays, are classified as background. The background samples of W + jets, Drell–Yan, diboson, and single-top-quark events are generated using MadGraph [22] or POWHEG [23], and showered and fragmented using PYTHIA 6.4.22 [24]. Next-to-leading order (NLO) cross sections are used for all background samples.

For both signal and background events, multiple pp interactions in the same or nearby bunch crossings (pileup) are simulated using PYTHIA and superimposed on the hard collision. Events are then simulated using a Geant4-based model [25] of the CMS detector, and finally reconstructed and analyzed with the same software used to process collision data.

The trigger efficiency for dilepton events that pass the analysis selection criteria is determined using a tag-and-probe method [26]. For the ee, $e\mu$, and $\mu\mu$ channels this gives p_{T}- and η-dependent efficiencies of approximately 100%, 95%, and 90%, respectively [27]. These efficiencies are used to weight the simulated events to account for the trigger requirement. The lepton selection efficiencies (reconstruction, identification, and isolation) are consistent between the data and the simulation [26, 28]. To account for the difference between the b-tagging efficiencies in data and simulation [19], data-to-simulation scale factors are applied for each jet in the simulated events. CMS studies [29] have shown that the top-quark p_{T} distribution in data is softer than in the NLO simulation. Reweighting the top-quark p_{T} in the simulation to match the data improves the modeling of the lepton and jet p_{T} distributions, and is applied to the MC@NLO $t\bar{t}$ sample used in this Letter. Due to the dependence of the spin correlations on the $t\bar{t}$ invariant mass, and thus the top-quark p_{T}, the p_{T} reweighting increases the fraction of top-quark pairs with aligned spins in the simulation. The simulation is used only for the unfolding, which is primarily sensitive to changes in acceptance, where the effect of the p_{T} reweighting largely cancels in the ratio. However, the top-quark p_{T} spectrum modeling remains as one of the most significant uncertainties.

After all weights are applied, a total of 740 background events are expected. There are 9824 events observed in data, and the remaining 9084 events are assumed to be signal (dileptonic $t\bar{t}$). The mean acceptance for signal events is 18%, and describes the fraction of all produced signal events that are expected to be selected.

While the $\Delta\phi_{\ell^+\ell^-}$ measurement relies purely on leptonic information, the measurements based on θ_ℓ require reconstruction of the entire $t\bar{t}$ system. Each event has two neutrinos, and there is also ambiguity in combining b jets with leptons, resulting in up to 16 possible solutions for the $t\bar{t}$ system. The analytical matrix weighting technique (AMWT) [30] is used to find the most probable solution, assuming a top-quark mass of 172.5 GeV. In events with only one b-tagged jet, the second b jet is assumed to be the untagged jet with the largest p_{T}. Solutions are assigned a weight, based on the probability of observing such a configuration, and the $t\bar{t}$ kinematic quantities are taken from the solution with the largest weight. To improve the efficiency of the technique in the presence of mismeasured jets, the solution for each event is integrated over parameterized jet and $E_{\mathrm{T}}^{\mathrm{miss}}$ resolution functions. Despite this, no solutions are found for approximately 14% of events, both in data and in the simulation. Events with no solutions are not used in the measurement of θ_ℓ. This is accounted for as an additional event selection requirement.

The backgrounds from Drell–Yan production and events with a misidentified lepton are estimated using both control data samples and simulation. The results agree within their uncertainties. Contributions to the background from single-top-quark and diboson events are estimated from simulation only. The simulation is chosen as the method to predict the background event yields and shapes, with systematic uncertainties based on comparisons with the estimates using data.

The Drell–Yan background outside of the Z-boson mass window is estimated using the ratio of simulated events inside/outside of the window to scale the observed event yield inside of the window. The contribution in this region from other processes, where the two leptons do not come from a Z boson, is estimated from $e\mu$ data and subtracted prior to performing the scaling.

The background with at least one misidentified lepton (non-dileptonic $t\bar{t}$, W+jets, and QCD) is estimated from control samples in data using a parametrization of the probability for a jet to be misidentified as a lepton. This parametrization is determined from data using events collected by jet triggers with varying energy thresholds. For both electrons and muons, an associated "loose" lepton candidate is defined based on relaxed isolation requirements. Lepton misidentification rates are parametrized as a function of lepton p_{T} and η, and are applied as weights to events containing exactly one fully-selected lepton candidate and one or more loose lepton candidates.

The measured distributions are distorted from the true underlying distributions by the limited acceptance of the detector and the finite resolution of the measurements. In order to correct the data for these effects, we apply an unfolding procedure, which yields the parton-level distributions of the variables under study, where the full covariance matrix is used to evaluate the uncertainties and bin-to-bin correlations.

The background-subtracted measured distribution $\vec{b}$ is related to the underlying parton-level distribution $\vec{x}$ by the matrix equation $\vec{b} = SA\vec{x}$, where A is a diagonal matrix describing the acceptance in each bin of the measured distribution, and S is a non-diagonal smearing matrix describing the migration of events between bins due to the finite detector resolution and reconstruction techniques. The A and S matrices are modeled using MC@NLO $t\bar{t}$ simulation.

We employ a regularized unfolding algorithm using the singular value decomposition method [31]. The effects of large statistical fluctuations in the algorithm are greatly reduced by introducing a regularization term in the unfolding procedure. The unfolding procedure is validated using pseudo-experiments by verifying the pull distributions and linearity for the observables under study.

Various systematic uncertainties affect the measurements. These are mainly related to the performance of the detector, and the modeling of the signal and background processes.

The uncertainty due to the jet energy scale (JES) corrections affects the AMWT $t\bar{t}$ solutions as well as the event selection. It is estimated by varying the JES of jets within their uncertainties, with the proper propagation to the $E_{\mathrm{T}}^{\mathrm{miss}}$. The uncertainty in the lepton energy scale, which affects mainly the lepton p_{T} distributions, is estimated by varying the energy scale of electrons by 0.5% (the uncertainty in muon energies is negligible in comparison), as estimated from comparisons between data and simulated Z-boson events.

The uncertainty in the background subtraction is obtained by making variations of the normalization of each background component, by 50% for single-top-quark and diboson production, and by 100% for the backgrounds from Drell–Yan production and from misidentified leptons.

The $t\bar{t}$ modeling and simulation uncertainties are evaluated by re-deriving the A and S matrices using simulated events with variations in the parameter of interest: the factorization and renormalization scales are together varied up and down by a factor of 2; the top-quark mass is varied by ± 3 GeV around $m_t = 172.5$ GeV; the parton distribution functions (PDFs) are varied using the PDF4LHC formula [32]; the jet energy resolution is varied by 5 to 10%, depending on the η of the jet; the simulated pileup multiplicity distribution is changed within its uncertainty; and the scale factors between data and simulation for b-tagging efficiency, trigger efficiency, and

lepton selection efficiency are shifted up and down by 1σ. In the simulated $t\bar{t}$ events, the τ spin is not propagated correctly to its decay products. This affects the angular distributions of the electrons and muons coming from τ decays. The corresponding systematic effect is estimated by reweighting the τ decay distributions to reproduce the SM expectations. A 100% systematic uncertainty is applied to the top-quark p_{T} reweighting, since the origin of the effect is not yet fully understood, and the resulting systematic uncertainty is quoted separately.

Finally, the results of the unfolding linearity tests are used to estimate the systematic uncertainty in the unfolding procedure. The contributions to the total systematic uncertainty (from their sum in quadrature) for each asymmetry variable are presented in Table I.

TABLE I. Systematic uncertainties in the background-subtracted and unfolded values of $A_{\Delta\phi}$, $A_{c_1c_2}$, and A_P.

Asymmetry variable	$A_{\Delta\phi}$	$A_{c_1c_2}$	A_P
Jet energy scale	0.002	0.012	0.009
Lepton energy scale	0.001	0.001	0.001
Background	0.003	0.001	0.006
Fact. and renorm. scales	0.001	0.010	0.004
Top-quark mass	0.002	0.009	0.016
Parton distribution functions	0.002	0.002	0.001
Jet energy resolution	< 0.001	< 0.001	< 0.001
Pileup	0.002	0.002	0.004
b-tagging scale factor	< 0.001	< 0.001	0.001
Lepton selection	< 0.001	< 0.001	< 0.001
τ decay polarization	0.001	0.002	0.001
Unfolding	0.004	0.020	0.002
Total systematic uncertainty	0.007	0.027	0.020
Top p_{T} reweighting uncertainty	0.012	0.010	0.008

The background-subtracted and unfolded distributions for $\Delta\phi_{\ell^+\ell^-}$, $\cos(\theta_{\ell^+})\cos(\theta_{\ell^-})$, and $\cos(\theta_\ell)$ are shown in Fig. 1, normalized to unity so that they represent parton-level differential cross sections in each variable. The data are compared to the predictions of the MC@NLO $t\bar{t}$ sample (with no data-derived reweighting applied), and to NLO calculations for $t\bar{t}$ production with and without spin correlation [12, 33].

The asymmetries determined from the unfolded distributions are also parton-level quantities, and are measured to be $A_{\Delta\phi} = 0.113 \pm 0.010 \pm 0.007 \pm 0.012$, $A_{c_1c_2} = -0.021 \pm 0.023 \pm 0.027 \pm 0.010$, and $A_P = 0.005 \pm 0.013 \pm 0.020 \pm 0.008$, where the uncertainties are statistical, systematic, and from top-quark p_{T} reweighting, respectively. These results are compared to the simulated and theoretical [12, 33] values in Table II. The $A_{\Delta\phi}$ result indicates the presence of $t\bar{t}$ spin correlations, and strongly disfavors the uncorrelated case.

In summary, this Letter presents measurements related to $t\bar{t}$ spin correlations and the top-quark polarization in the $t\bar{t}$ dilepton final states (e^+e^-, $\mu^+\mu^-$, and $e^\pm\mu^\mp$), using asymmetry distributions unfolded to the parton level. The results are in agreement with the standard model predictions for all three measured variables.

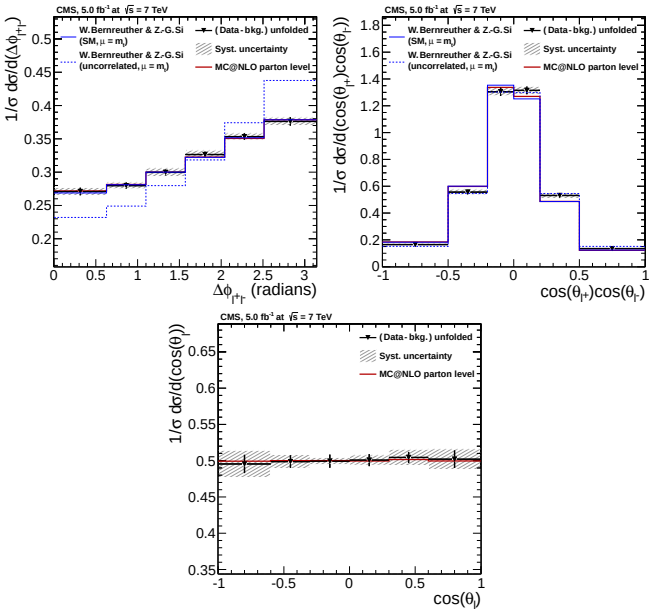

FIG. 1. Background-subtracted and unfolded differential cross sections for $\Delta\phi_{\ell^+\ell^-}$, $\cos(\theta_{\ell^+})\cos(\theta_{\ell^-})$, and $\cos(\theta_\ell)$. The error bars represent statistical uncertainties only, while the systematic uncertainty band is represented by the hatched area. The bin contents are correlated due to the unfolding.

We would like to thank Prof. W. Bernreuther and Prof. Z.-G. Si for calculating the theoretical predictions of Fig. 1 and Table II for this Letter. We congratulate our colleagues in the CERN accelerator departments for the excellent performance of the LHC and thank the technical and administrative staff at CERN and at other CMS institutes for their contributions to the success of the CMS effort. In addition, we gratefully acknowledge the computing centres and personnel of the Worldwide LHC Computing Grid for delivering so effectively the computing infrastructure essential to our analyses. Finally, we acknowledge the enduring support for the construction and operation of the LHC and the CMS detector provided by the following funding agencies: BMWF and FWF (Austria); FNRS and FWO (Belgium); CNPq, CAPES, FAPERJ, and FAPESP (Brazil); MES (Bulgaria); CERN; CAS, MoST, and NSFC (China); COLCIENCIAS (Colombia); MSES (Croatia); RPF (Cyprus); MoER, SF0690030s09 and ERDF (Estonia); Academy of Finland, MEC, and HIP (Finland); CEA and CNRS/IN2P3 (France); BMBF, DFG, and HGF (Germany); GSRT (Greece); OTKA and NIH (Hungary); DAE and DST (India); IPM (Iran); SFI (Ireland); INFN (Italy); NRF and WCU (Republic of Korea); LAS (Lithuania); CINVESTAV, CONACYT, SEP, and UASLP-FAI (Mexico); MBIE (New

TABLE II. Parton-level asymmetries. The uncertainties in the unfolded results are statistical, systematic, and the additional uncertainty from the top-quark p_{T} reweighting. The uncertainties in the simulated results are statistical only, while the uncertainties in the NLO calculations for correlated and uncorrelated $t\bar{t}$ spins come from scale variations up and down by a factor of two. The prediction for $A_{c_1c_2}$ is exactly zero in the absence of spin correlations by construction.

Asymmetry	Data (unfolded)	MC@NLO	NLO (SM, correlated)	NLO (uncorrelated)
$A_{\Delta\phi}$	$0.113 \pm 0.010 \pm 0.007 \pm 0.012$	0.110 ± 0.001	$0.115^{+0.014}_{-0.016}$	$0.210^{+0.013}_{-0.008}$
$A_{c_1c_2}$	$-0.021 \pm 0.023 \pm 0.027 \pm 0.010$	-0.078 ± 0.001	-0.078 ± 0.006	0
A_P	$0.005 \pm 0.013 \pm 0.020 \pm 0.008$	0.000 ± 0.001	N/A	N/A

Zealand); PAEC (Pakistan); MSHE and NSC (Poland); FCT (Portugal); JINR (Dubna); MON, RosAtom, RAS and RFBR (Russia); MESTD (Serbia); SEIDI and CPAN (Spain); Swiss Funding Agencies (Switzerland); NSC (Taipei); ThEPCenter, IPST, STAR and NSTDA (Thailand); TUBITAK and TAEK (Turkey); NASU (Ukraine); STFC (United Kingdom); DOE and NSF (USA).

[1] M. Beneke *et al.*, "Top Quark Physics," (2000), arXiv:hep-ph/0003033 [hep-ph].
[2] D. Krohn, T. Liu, J. Shelton, and L.-T. Wang, Phys. Rev. D **84**, 074034 (2011), arXiv:1105.3743 [hep-ph].
[3] CDF and D0 Collaborations, Phys. Rev. D **86**, 092003 (2012), an update can be found in arXiv:1305.3929, arXiv:1207.1069 [hep-ex].
[4] J. Beringer *et al.* (Particle Data Group), Phys. Rev. D **86**, 010001 (2012 and 2013 partial update for the 2014 edition).
[5] G. Mahlon and S. Parke, Phys. Rev. D **81**, 074024 (2010), arXiv:1001.3422 [hep-ph].
[6] T. Aaltonen *et al.* (CDF), Phys. Rev. D **83**, 031104 (2011), arXiv:1012.3093 [hep-ex].
[7] V. M. Abazov *et al.* (D0), Phys. Rev. Lett. **107**, 032001 (2011), arXiv:1104.5194 [hep-ex].
[8] V. M. Abazov *et al.* (D0), Phys. Lett. B **702**, 16 (2011), arXiv:1103.1871 [hep-ex].
[9] G. Aad *et al.* (ATLAS), Phys. Rev. Lett. **108**, 212001 (2012), arXiv:1203.4081 [hep-ex].
[10] V. M. Abazov *et al.* (D0), Phys. Rev. D **87**, 011103 (2013), arXiv:1207.0364 [hep-ex].
[11] G. Aad *et al.* (ATLAS), submitted to Phys. Rev. Lett. (2013), arXiv:1307.6511 [hep-ex].
[12] W. Bernreuther and Z.-G. Si, Phys. Lett. B **725**, 115 (2013), arXiv:1305.2066 [hep-ph].
[13] S. Chatrchyan *et al.* (CMS), JINST **3**, S08004 (2008).
[14] CMS Collaboration (CMS), *Electron Reconstruction and Identification at* $\sqrt{s} = 7$ *TeV*, CMS Physics Analysis Summary CMS-PAS-EGM-10-004 (2010).
[15] S. Chatrchyan *et al.* (CMS), JINST **7**, P10002 (2012), arXiv:1206.4071 [physics.ins-det].
[16] CMS Collaboration (CMS), *Commissioning of the Particle-Flow Reconstruction in Minimum-Bias and Jet Events from pp Collisions at 7 TeV*, CMS Physics Analysis Summary CMS-PAS-PFT-10-002 (2010).
[17] M. Cacciari, G. P. Salam, and G. Soyez, JHEP **04**, 063 (2008), arXiv:0802.1189 [hep-ph].
[18] S. Chatrchyan *et al.* (CMS), JINST **6**, P11002 (2011), arXiv:1107.4277 [physics.ins-det].
[19] S. Chatrchyan *et al.* (CMS), JINST **8**, P04013 (2013), arXiv:1211.4462 [hep-ex].
[20] S. Frixione and B. R. Webber, JHEP **06**, 029 (2002), hep-ph/0204244.
[21] G. Corcella *et al.*, JHEP **01**, 010 (2001), arXiv:hep-ph/0011363.
[22] J. Alwall, M. Herquet, F. Maltoni, O. Mattelaer, and T. Stelzer, JHEP **06**, 128 (2011), arXiv:1106.0522 [hep-ph].
[23] S. Frixione, P. Nason, and C. Oleari, JHEP **11**, 070 (2007), arXiv:0709.2092 [hep-ph].
[24] T. Sjöstrand, S. Mrenna, and P. Skands, JHEP **05**, 026 (2006), arXiv:hep-ph/0603175.
[25] S. Agostinelli *et al.* (GEANT4), Nucl. Instrum. Meth. A **506**, 250 (2003).
[26] S. Chatrchyan *et al.* (CMS), JHEP **10**, 007 (2011), arXiv:1108.0566 [hep-ex].
[27] S. Chatrchyan *et al.* (CMS), Phys. Lett. B **716**, 103 (2012), arXiv:1203.5410 [hep-ex].
[28] S. Chatrchyan *et al.* (CMS), JHEP **11**, 067 (2012), arXiv:1208.2671 [hep-ex].
[29] S. Chatrchyan *et al.*, Eur. Phys. J. C **73**, 1 (2013), arXiv:1211.2220 [hep-ex].
[30] S. Chatrchyan *et al.* (CMS), JHEP **07**, 049 (2011), arXiv:1105.5661 [hep-ex].
[31] A. Hoecker and V. Kartvelishvili, Nucl. Instrum. Meth. A **372**, 469 (1996), arXiv:hep-ph/9509307 [hep-ph].
[32] M. Botje *et al.*, "The PDF4LHC Working Group Interim Recommendations," arXiv:1101.0538 [hep-ph].
[33] W. Bernreuther and Z.-G. Si, Nuc. Phys. B **837**, 90 (2010), and private communication, arXiv:1003.3926 [hep-ph].